Momentum-space treatment of Coulomb distortions in a multiple-scattering expansion

C. R. Chinn
Physics Department, Lawrence Livermore National Laboratory, Livermore, California 94550

Ch. Elster
Department of Physics, Ohio State University, Columbus, Ohio 43210

R. M. Thaler
Los Alamos National Laboratory, Los Alamos, New Mexico 87545
and Department of Physics, Case Western Reserve University, Cleveland, Ohio 44106
(Received 13 May 1991)

The momentum-space treatment of the Coulomb interaction within the framework of the Watson multiple-scattering expansion is derived and tested numerically. By neglecting virtual Coulomb excitations and higher-order terms, the lowest-order optical potential for proton-nucleus scattering is shown to be the sum of the convolutions of a two-body nucleon-nucleon t matrix with the nuclear density and the point Coulomb interaction with the nuclear charge density. The calculation of the optical potential, as well as the treatment of the Coulomb interaction, is performed entirely in momentum space in an exact and numerically stable procedure. Elastic-scattering observables are presented for ^{16}O, ^{40}Ca, and ^{208}Pb at energies up to 500 MeV. Comparisons are made with approximate treatments of the Coulomb interaction. The interference of nonlocality effects in the nuclear optical potential with different treatments of the Coulomb interaction is investigated.

I. INTRODUCTION

The theory of the nucleon-nucleus optical potential continues to play an important role in nuclear physics. It is one of the simplest and yet most powerful tools available for describing and understanding the physics involved in nucleon-nucleus scattering. Recent papers have demonstrated that significant improvement in the description of spin observables for elastic proton scattering from nuclei is obtained within a nonrelativistic framework by including the nonlocal structure of the first-order optical potential [1–4]. Though these works differ in the underlying nucleon-nucleon (NN) interaction, the sophistication with which the NN interaction is convoluted with the nuclear density matrix and other calculational details, it has been generally found that nonlocalities in the first-order optical potential are non-negligible.

The nonlocal and off-shell features of the optical potential are more readily obtained in a momentum-space representation, where the scattering calculations are most conveniently performed by solving a Lippman-Schwinger-type integral equation. Unfortunately, a long-standing handicap of proton-nucleus scattering calculations in momentum space has been the lack of consistent and reliable methods for treating charged, strongly interacting particles.

The issues to be dealt with in a proton-nucleus calculation using a multiple-scattering approach in momentum space are twofold. First, there is the obvious difficulty given by the $1/q^2$ singularity of the Coulomb interaction. Recently, several different methods have been proposed to deal with the Coulomb singularity in momentum space [1,5–8]. Some of these methods use an extraneous cutoff built into the calculation to constrain the singular behavior of the Coulomb interaction. These methods are, in principle, exact; however, the cutoff can never truly be taken to the limit. The original method of Vincent and Phatak [5] is of this character, and its numerical stability has been found to be very difficult to control, since the procedure is sensitive to the cutoff parameter. Recently proposed refinements of this method [6,7] reduce that sensitivity.

We have proposed a method in which the limits of the cutoff are taken analytically and no cutoff parameters appear in the numerical calculations [8]. This procedure is exact and is not limited to a specific energy or charge in its range of application. In Ref. [8], this method has been explored mathematically and numerically with a simple potential whose Fourier transform exists analytically, and has been demonstrated to be stable and accurate. In this paper we use which procedure to calculate elastic proton-nucleus scattering observables.

The second issue to be discussed in this treatment of the Coulomb interaction in a multiple-scattering expansion. Two standard and equivalent approaches for defining an optical potential are the multiple-scattering formulations of Watson [9] and Kerman, McManus, and Thaler (KMT) [10]. These and other similar presentations contain no explicit treatment of the Coulomb interaction. For practical microscopic analyses of intermediate-energy proton-nucleus scattering the Watson and KMT approaches are most often used, and the Coulomb interaction is generally included according to some arbitrary prescription. In Ref. [11], a scheme has been suggested to include the Coulomb interaction within the KMT formalism in an approximate fashion. We do

not follow this line but rather start from the Watson approach and show, that under the assumption of neglecting Coulomb excitations, the generally applied prescriptions are theoretically justified.

The structure of the paper is as follows: In Sec. II we introduce the multiple-scattering expansion with nuclear and Coulomb interactions. We then isolate the relevant Coulomb and nuclear terms for a first-order optical potential. In Sec. III we describe the calculation of Coulomb distorted nuclear matrix elements. The calculation of proton-nucleus elastic-scattering observables and a comparison with approximate treatments of Coulomb distortions are presented in Sec. IV. We also compare the size of off-shell effects for a heavy nucleus (^{208}Pb) to those present in lighter nuclei (^{40}Ca). Our conclusions are presented in Sec. V.

II. MULTIPLE-SCATTERING THEORY FOR CHARGED PARTICLES

The incorporation of both nuclear and Coulomb effects in medium-energy scattering is made awkward by the fact that the long-range Coulomb interaction calls for an essentially adiabatic treatment, whereas the short-range nuclear part is best treated as impulsive. Here we present a formulation of the problem of elastic scattering of protons from nuclei, which incorporates the different characters of the interactions in a theoretically consistent fashion. The basic ingredient of this formulation is the application of the familiar two-potential formula in a multiple-scattering theory.

The transition amplitude T for proton-nucleus scattering is expressed by the Lippmann-Schwinger equation

$$T=V+VG_0T \tag{1}$$

or

$$T=V+VGV\ . \tag{2}$$

The energy-independent potential V for proton-nucleus scattering with two-body forces is the sum of nuclear and Coulomb interactions,

$$V=V^N+V^C=\sum_{i=1}^{A}v_{0i}+\sum_{i=1}^{Z}V_{0i}^C\ . \tag{3}$$

Here v_{0i} and V_{0i}^C are the interactions between the projectile and the ith particle. The Green's functions G and G_0 are given by

$$\begin{aligned} G_0^{-1}(E)&=E-h_0-H_A\ ,\\ G^{-1}(E)&=E-h_0-H_A-V\ , \end{aligned} \tag{4}$$

where H_A (the target Hamiltonian) is defined as

$$H_A=\sum_{i=1}^{A}h_i+\sum_{i<j}^{A}V_{ij}\ . \tag{5}$$

The convention we have used is that V_{ij} represents the two-body potential between nucleons i and j, including both the short-range nuclear and long-range Coulomb force. The symbol h_i stands for the kinetic-energy operator for particle i.

We begin with a projection operator P, defined in the usual way, such that P projects onto the nuclear target ground state $|\Phi_A\rangle$, i.e.,

$$P=\frac{|\Phi_A\rangle\langle\Phi_A|}{\langle\Phi_A|\Phi_A\rangle}\ . \tag{6}$$

For elastic scattering, we need only the operator PTP, rather than the full T. We now proceed to split the external interaction V of Eq. (3) into two parts, as

$$\begin{aligned} V&=PV^CP+\left[\sum_{i=1}^{A}v_{0i}+QV^CP+PV^CQ+QV^CQ\right]\\ &\equiv PV^CP+\{\overline{W}\}\ , \end{aligned} \tag{7}$$

where Q is complementary to P. The operator PV^CP represents the Coulomb interaction on the projectile due to the static charge distribution of the nuclear target.

In the present treatment we ignore excitations of the nuclear target in the Coulomb interaction, i.e., we take $V^CQ=QV^C=0$, so that $\overline{W}$ contains only strong-interaction terms

$$\overline{W}\cong\sum_{i=1}^{A}v_{0i}\ . \tag{8}$$

At this point, the short-range part of the Coulomb interaction due to the finite size of the nucleus is separated out and included into $\overline{W}$, leaving the long-range point Coulomb interaction PV_p^CP and short-ranged interactions $\overline{W}$. We then rewrite Eq. (7) as

$$\begin{aligned} V&=PV_p^CP+\left[\sum_{i=1}^{A}v_{0i}+(P[V^C-V_p^C]P)\right]\\ &=PV_p^CP+\left[\sum_{i=1}^{A}v_{0i}+(\overline{V}^C)\right]\\ &=PV_p^CP+\{W\}\ . \end{aligned} \tag{9}$$

Here Eq. (9) series to define $\overline{V}^C$ and W, and we note that W is of finite range. The point Coulomb interaction V_p^C is given in coordinate space by Ze^2/r_0, where r_0 is the coordinate of the projectile relative to the center of mass of the target nucleus. The short-ranged Coulomb contribution $\overline{V}^C$ represents the difference between the Coulomb interaction folded over the finite-range density distribution and the point Coulomb potential.

By defining the Coulomb Green's function G_C as

$$G_C^{-1}=E-h_0-H_A-PV_p^CP\ , \tag{10}$$

we find for the point Coulomb transition operator

$$PT^CP=PV_p^CP+PV_p^CPG_0PT^CP\ . \tag{11}$$

Applying the two-potential formula to Eq. (1) and using V as given in Eq. (9) in conjunction with Eq. (11) yields, for the transition amplitude T,

$$T=PT^CP+\Omega_C^{(-)\dagger}W\Omega^{(+)}\ , \tag{12}$$

with the Møller operators given by

$$\Omega = 1 + GV$$
$$= [1 + GW]\Omega_C \tag{13}$$

and

$$\Omega_C = 1 + G_0 P V_p^C P \Omega_C$$
$$= 1 + G_C P V_p^C P \ . \tag{14}$$

With these preliminaries established and with the aid of Eq. (13), we may rewrite Eq. (12) as

$$T = PT^C P + \Omega_C^{(-)\dagger}[W + WGW]\Omega_C^{(+)}$$
$$\equiv PT^C P + \Omega_C^{(-)\dagger}\mathcal{T}\Omega_C^{(+)} \ , \tag{15}$$

where $\mathcal{T}$ is given by

$$\mathcal{T} = W + WGW \tag{16}$$

or equivalently by

$$\mathcal{T} = W + WG_C\mathcal{T} \ . \tag{17}$$

In the context of elastic scattering we are interested in the operator

$$PTP = PT^C P + P\Omega_C^{(-)\dagger}P[P\mathcal{T}P]P\Omega_C^{(+)}P \ , \tag{18}$$

hence, we need only to consider

$$P\mathcal{T}P = PWP + PWGWP \tag{19}$$

or

$$\mathcal{T} = W + WG_C\mathcal{T} \ . \tag{20}$$

If we define an optical potential $\tilde{U}$ in the usual way such that

$$\mathcal{T} = \tilde{U} + \tilde{U}G_C P\mathcal{T} \ , \tag{21}$$

then it follows immediately that

$$\tilde{U} = W + WG_C Q\tilde{U} \ . \tag{22}$$

The definition of G_C, Eq. (10), then yields

$$G_C Q = G_0 Q \ , \tag{23}$$

so that

$$\tilde{U} = W + WG_0 Q\tilde{U} \ . \tag{24}$$

In order to make contact with an optical potential as it is usually defined in the Watson or KMT formulation of the multiple-scattering expansion, we define a nuclear optical potential as

$$U^N = V^N + V^N G_0 Q U^N \ . \tag{25}$$

We then find

$$\tilde{U} = U^N + (1 + U^N G_0 Q)\bar{V}^C(1 + G_0 Q\tilde{U}) \ . \tag{26}$$

Since $Q\bar{V}^C = \bar{V}^C Q = 0$, the above equation reduces to our final expression for the optical potential

$$\tilde{U} = U^N + \bar{V}^C \ . \tag{27}$$

This shows that the first-order optical potential $\tilde{U}$ is given by a nuclear optical potential U^N and a short-ranged Coulomb interaction $\bar{V}^C$ as defined in Eq. (9).

We now return to the consideration of U^N as given in Eq. (25). If we express U^N as

$$U^N = \sum_{i=1}^{A} U_i \ , \tag{28}$$

it follows that

$$U_i = v_{0i} + v_{0i}G_0 Q U_i + v_{0i}G_0 Q \sum_{j \neq i} U_j \ . \tag{29}$$

If we define an operator τ_i as

$$\tau_i = v_{0i} + v_{0i}G_0 Q\tau_i \ , \tag{30}$$

we obtain

$$U_i = \tau_i + \tau_i G_0 Q \sum_{j \neq i} U_j \ . \tag{31}$$

Here we see that Eq. (31) represents the well-known Watson multiple-scattering expansion for the optical potential [9]. Its first-order term, the "impulse" approximation to U_i is given by τ_i. Since we are interested in PUP, and hence $P\tau_i P$, we can apply completeness $(P + Q = 1)$ to express $P\tau_i P$ as

$$P\tau_i P = Pt_i P - Pt_i PG_0 P\tau_i P \ , \tag{32}$$

where t_i is given by

$$t_i = v_{0i} + v_{0i}G_0 t_i \ . \tag{33}$$

It should be noted that the definition of t_i does not contain any projector Q and that it can thus more readily be related to the free two-nucleon transition operator. In the case of a purely strong interaction, the insertion of Eq. (33) into Eq. (24) leads, after some algebraic manipulations, to the well-known KMT formulation of the multiple-scattering expansion [10]. The equivalence of the first-order optical potential in the KMT and the Watson formulation of a multiple-scattering expansion for the case of a purely nuclear interaction has been shown in Ref. [12]. However, in the presence of an additional Coulomb interaction, this manipulation cannot be performed in the same way without leading to inconsistencies. We point out that Eq. (32) is a one-body integral equation with a structure similar to the scattering equation, Eq. (1). Therefore, its numerical solution does not impose any additional difficulties on the solution of the scattering problem. We obtain the first-order optical potential by solving Eq. (32) numerically.

Our principal task now becomes finding a reliable procedure to obtain $Pt_i P$. The free two-nucleon transition operator t_{0i} is given by

$$t_{0i}(E') = v_{0i} + v_{0i}g_0(E')t_{0i}(E') \ , \tag{34}$$

where the two-nucleon propagator g_0 is

$$g_0^{-1} = E' - h_0 - h_i + i\varepsilon \ . \tag{35}$$

The energy E' is the energy of the two free nucleons in the frame, where one is at rest. From the comparison of

Eqs. (34) and (33), we see that

$$t_i = t_{0i}(E') + t_{0i}(E')[G_0 - g_0(E')]t_i$$
$$= t_{0i}(E') + t_{0i}(E')g_0(E')(E' - E + H_A - h_i)G_0 t_i \ . \tag{36}$$

The second term on the right-hand side in Eq. (36) contains effects of the nuclear medium on the propagator. Various prescriptions have been put forth as to the "best" choice of E' so as to minimize the effect of the nuclear medium. The best choice for E' is still an open question [14].

III. CALCULATION OF THE TRANSITION AMPLITUDES

In the previous section we have established the general formalism for treating consistently the nuclear and the Coulomb parts of the external interaction in a multiple-scattering expansion. The approximations, which lead to the first-order optical potential in a Watson-type rearrangement of the multiple-scattering series, have been presented. The elastic proton-nucleus scattering T-matrix element, Eq. (18), can be written explicitly as

$$\langle \mathbf{k}'\Phi_A | T | \mathbf{k}\Phi_A \rangle = \langle \mathbf{k}'\Phi_A | T^C | \mathbf{k}\Phi_A \rangle + \langle \psi_C^{(-)}(\mathbf{k}')\Phi_A | \mathcal{T} | \psi_C^{(+)}(\mathbf{k})\Phi_A \rangle \ , \tag{37}$$

where the $|\psi_C^{(\pm)}(\mathbf{k})\rangle$ are Coulomb distorted wave functions. Since we restrict ourselves to considering the lowest-order term in the multiple-scattering expansion [Eqs. (24) and (31)], we have for $\hat{T}$,

$$\hat{T} = \hat{U} + \hat{U} G_C \hat{T} \ , \tag{38}$$

where we define

$$\hat{U} \equiv \langle \Phi_A | \tilde{U} | \Phi_A \rangle = \sum_i \langle \Phi_A | \tau_i | \Phi_A \rangle + \langle \Phi_A | \bar{V}^C | \Phi_A \rangle \ ,$$
$$\hat{T} \equiv \langle \Phi_A | \mathcal{T} | \Phi_A \rangle \ . \tag{39}$$

The operator τ_i is related to the free two-nucleon transition operator t_i as given in Eq. (32), which takes the explicit form

$$\langle \Phi_A | \tau_i | \Phi_A \rangle = \langle \Phi_A | t_{0i} | \Phi_A \rangle - \langle \Phi_A | t_{0i} | \Phi_A \rangle \times \frac{1}{E - h_0 + i\varepsilon} \langle \Phi_A | \tau_i | \Phi_A \rangle \ . \tag{40}$$

At this point we do not need to specify the calculation of $\langle \Phi_A | t_i | \Phi_A \rangle$, this has been studied in detail elsewhere [1–4]. The $t\rho$-type matrix element may be obtained by a full-folding procedure [1,2,4] or by an approximation to it. After having obtained $t\rho$, we calculate the Watson-type $\tau\rho$ by solving Eq. (40). This leads to the optical potential $\hat{U}$ shown in Eq. (39). We then need to solve for the scattering matrix element $\langle \psi_C^{(-)}(\mathbf{k}') | \hat{T} | \psi_C^{(+)}(\mathbf{k}) \rangle$ as displayed in Eqs. (37) and (38). To this end we solve the equation

$$\langle \psi_C^{(-)}(\mathbf{k}') | \hat{T} | \psi_C^{(+)}(\mathbf{k}) \rangle = \langle \psi_C^{(-)}(\mathbf{k}') | \hat{U} | \psi_C^{(+)}(\mathbf{k}) \rangle + \int \langle \psi_C^{(-)}(\mathbf{k}') | \hat{U} | \psi_C^{(+)}(\mathbf{k}'') \rangle \frac{d^3\mathbf{k}''}{E - E(k''^2) + i\varepsilon} \langle \psi_C^{(+)}(\mathbf{k}'') | \hat{T} | \psi_C^{(+)}(\mathbf{k}) \rangle \ . \tag{41}$$

It should be noted that the propagator takes this simple Lippmann-Schwinger-type form through the insertion of a complete set of Coulomb eigenfunctions. (It is assumed that there is no bound state present.) In the angular momentum decomposed form, we note that $\langle \psi_C^{(-)}(k') | = e^{2i\sigma_l} \langle \psi_C^{(+)}(k') |$, where σ_l is the so-called Coulomb phase shift, so that Eq. (41) becomes the standard Lippmann-Schwinger equation

$$\langle \mathbf{k}' | \bar{T} | \mathbf{k} \rangle = \langle \mathbf{k}' | \bar{U} | \mathbf{k} \rangle + \int \langle \mathbf{k}' | \bar{U} | \mathbf{k}'' \rangle \times \frac{d^3\mathbf{k}''}{E - E(k''^2) + i\varepsilon} \langle \mathbf{k}'' | \bar{T} | \mathbf{k} \rangle \ , \tag{42}$$

where

$$\langle \mathbf{k}' | \bar{T} | \mathbf{k} \rangle = \langle \psi_C^{(+)}(\mathbf{k}') | \hat{T} | \psi_C^{(+)}(\mathbf{k}) \rangle \ , \tag{43}$$

and

$$\langle \mathbf{k}' | \bar{U} | \mathbf{k} \rangle = \langle \psi_C^{(+)}(\mathbf{k}') | \hat{U} | \psi_C^{(+)}(\mathbf{k}) \rangle \ . \tag{44}$$

In order to solve Eq. (42), we need to be able to generate the momentum space matrix element $\langle \mathbf{k}' | \bar{U} | \mathbf{k} \rangle$ as given by Eq. (44). We begin with $\langle \mathbf{k}'\Phi_A | \sum_i \tau_i | \mathbf{k}\Phi_A \rangle$, which we obtain from the free $t\rho$ by means of Eq. (40). We transform this into coordinate space, through the double Fourier transform

$$\langle \mathbf{r}' | \hat{U} | \mathbf{r} \rangle = \int \langle \mathbf{r}' | \mathbf{k}' \rangle d^3\mathbf{k}' \langle \mathbf{k}' | \hat{U} | \mathbf{k} \rangle d^3\mathbf{k} \langle \mathbf{k} | \mathbf{r} \rangle \tag{45}$$

and then construct the matrix element of Eq. (44) by folding $\langle \mathbf{r}' | \hat{U} | \mathbf{r} \rangle$ with coordinate space Coulomb wave functions

$$\langle \mathbf{k}' | \bar{U} | \mathbf{k} \rangle = \int \langle \psi_C^{(+)}(\mathbf{k}') | \mathbf{r}' \rangle d^3\mathbf{r}' \langle \mathbf{r}' | \hat{U} | \mathbf{r} \rangle \times d^3\mathbf{r} \langle \mathbf{r} | \psi_C^{(+)}(\mathbf{k}) \rangle \ . \tag{46}$$

The reason for applying this procedure is that the Coulomb wave functions are well defined in coordinate space, whereas their counterparts in momentum space do not exist in a functional sense. The details and mathematical justifications for the above outlined procedure for treating Coulomb distortions in momentum space are carefully discussed in Ref. [8]. The actual cal-

culations of Eqs. (45) and (46) are time consuming, but this procedure is readily manageable with modern vectorized computers.

IV. NUMERICAL RESULTS AND DISCUSSION

We have applied the method discussed above to calculate proton-nucleus elastic-scattering observables for three closed-shell nuclei at several energies. Previously, we have shown [8] that this *exact* method is a completely reliable calculational scheme and tested it for certain simple cases for charges up to $Z=100$ and energies from 10 MeV to 1 GeV. Here we have applied this approach for predicting proton-nucleus elastic-scattering observables in the energy range from 100 to 500 MeV and charges from $Z=8$ to 82 in the context of first-order multiple-scattering theory. Again, we find the method completely straightforward and accurate.

We now examine the difference between these exact results and an approximate scheme used in previous works [3,4,13]. In these works, the calculation of the Coulomb distortion effect has been simplified by the replacement of the exact expression of Eq. (44) by the approximation

$$\langle k'|\bar{U}|k\rangle_l = \langle \psi_C^{(+)}(k')|\hat{U}|\psi_C^{(+)}(k)\rangle_l \approx \langle k'|\hat{U}|k\rangle_l , \quad (47)$$

where the subscript l indicates that an angular momentum decomposition has been performed. The two-

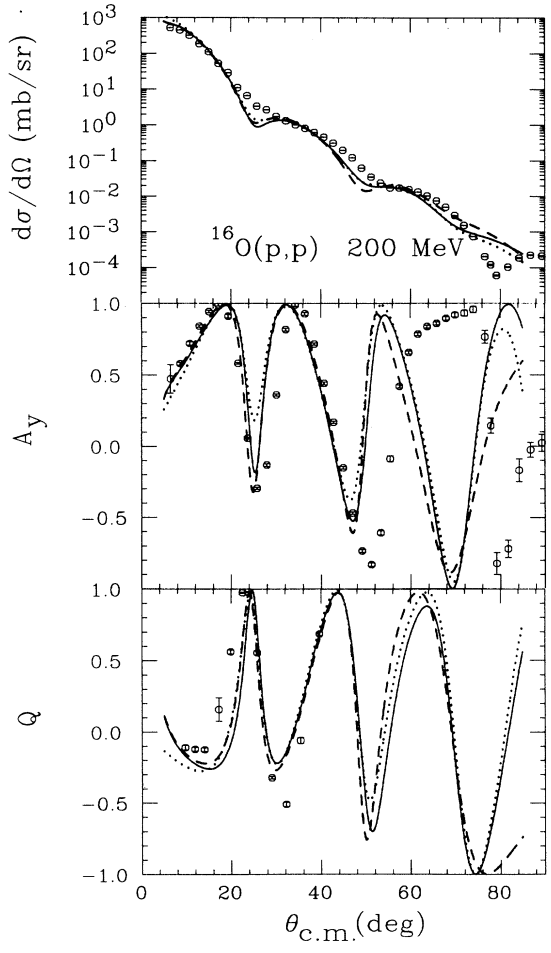

FIG. 1. The angular distribution of the differential cross section, analyzing power (A_y), and spin-rotation function (Q) for elastic proton scattering from ^{16}O at 200 MeV laboratory energy. The calculations are performed with a first-order optical potential obtained from the bull Bonn interaction in the optimum factorized approximation. The solid curve represents the exact treatment of the Coulomb distortions, whereas the dashed curve employs the PW approximation. The dotted line omits Coulomb contributions altogether. The data are from Ref. [20].

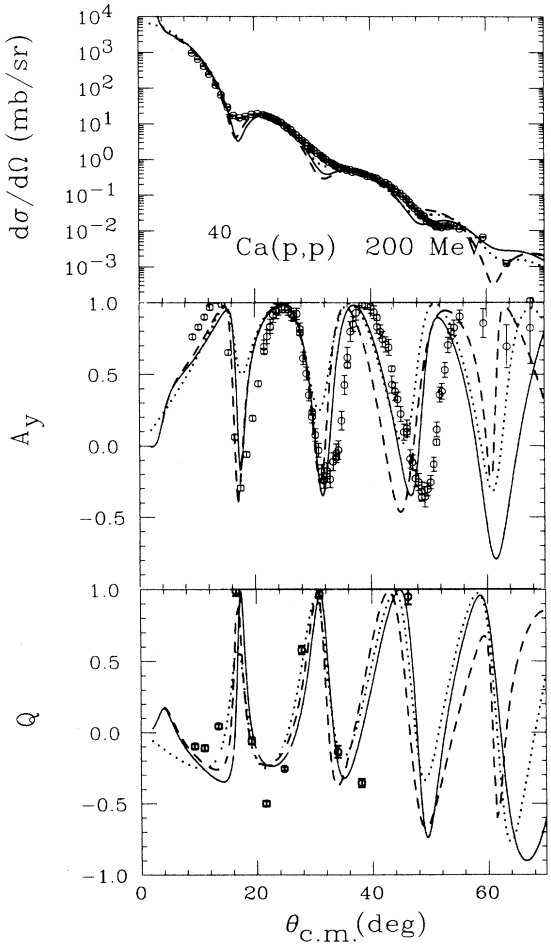

FIG. 2. The angular distribution of the differential cross section, A_y, and Q for elastic proton scattering from ^{40}Ca at 200 MeV laboratory energy. The calculations are performed with a first-order optical potential obtained from the full Bonn interaction in the optimum factorized approximation. The curves have the same meaning as in Fig. 1. The data are from Ref. [20].

potential formula in this case becomes

$$\langle k'\Phi_A|T|k\Phi_A\rangle_l=\langle k'\Phi_A|T^C|k\Phi_A\rangle_l + e^{2i\sigma_l}\langle\psi_C^{(+)}(k')|\hat{T}|\psi_C^{(+)}(k)\rangle_l \approx\langle k'\Phi_A|T^C|k\Phi_A\rangle_l + e^{2i\sigma_l}\langle k'|\hat{T}|k\rangle_l . \quad (48)$$

The approximation, Eq. (47) (which we henceforth refer to as the PW or plane-wave approximation), simply replaces the Coulomb distorted matrix element of the optical potential by its plane-wave counterpart. In other words, this means that the total phase shift δ_l, which is given by

$$\delta_l=\sigma_l+\delta_l^{\rm SR} , \quad (49)$$

where $\delta_l^{\rm SR}$ (the short-range phase shift with Coulomb distortions taken into account) is the difference between the full phase shift δ_l and the point Coulomb phase shift σ_l, is approximated by the choice

$$\delta_l^{\rm SR}\approx\tilde{\delta}_l^{\rm SR} . \quad (50)$$

The phase shift $\tilde{\delta}_l^{\rm SR}$ is calculated for the short-range (SR) force without the point Coulomb interaction. This short-range force includes the difference between the point Coulomb and the distributed Coulomb as well as the nuclear force. The PW approximation has been studied in a few cases [2,7], but in order to precisely quantify its range of validity, a study of various nuclei at different scattering energies is required and presented here.

In order to calculate the matrix element of the optical potential $\langle\mathbf{k}'|\hat{U}|\mathbf{k}\rangle$, given in Eq. (39), it is necessary to evaluate the matrix element $\langle\mathbf{k}'\Phi_A|t_{0i}|\mathbf{k}\Phi_A\rangle$ entering Eq. (40). This quantity represents the full-folding integral over the off-shell two-body nucleon-nucleon (*NN*) *t*-matrix and the nuclear density matrix. Its evaluation has been performed by several groups with different nuclear densities and *NN* interactions [1,2,4]. To simplify the calculations, we use the optimum factorized or off-shell $t\rho$ approximation [13], which has been found to be a good approximation to the full-folding integral in the energy regime between 200 and 800 MeV [2,4]. As shown in Eq. (36), the free *NN t* matrix has to be evaluated at an approximate energy E'. In principle, this energy should be the beam energy minus the kinetic energy of the center of mass in the interacting pair less the binding energy of the struck particle [14]. Since, in practice, the relevant-matrix elements do not depend strongly on this variable [15], E' is set to the two-body energy corresponding to free *NN* scattering at the beam energy. It is to be understood that all spin integrations are performed in obtaining $\langle\mathbf{k}'|\hat{U}|\mathbf{k}\rangle$ (under the usual assumption of a spin-saturated target) thus reducing the required *NN t* matrix elements to the spin-independent component (corresponding to Wolfenstein amplitude *A*) and the spin-orbit component (corresponding to Wolfenstein amplitude *C*). All scattering calculations presented here contain an additional factor in the optical potential to account for the transformation of the *NN t* matrix from the two -nucleon c.m. frame to the nucleon-nucleus c.m. frame. This Møller factor is obtained in a manner discussed in Ref. [13].

In Figs. 1–3 we show the angular distributions of the differential cross section, the analyzing power (A_y), and the spin rotation function (Q) for *p*-nucleus elastic scattering at 200 MeV laboratory energy for ^{16}O, ^{40}Ca, and ^{208}Pb. All calculations are carried out in the optimum factorized approximation. We employ the *NN t* matrix from the full Bonn interaction [16], which includes the effects of relativistic kinematics, retarded meson propagators as given by time-ordered perturbation theory, and crossed and iterative meson exchanges with *NN*, *N*Δ, and ΔΔ intermediate states. The densities of ^{16}O and ^{40}Ca are described by three-parameter Fermi shapes, derived from experimentally determined proton charge distributions, which are obtained from electron scattering [17]. For ^{208}Pb, the baryon densities are obtained from a microscopic Hartree-Fock-Bogoliubov calculation [18], where the finite-range D1S effective interaction of Gogny [19] is used. This interaction includes density-dependent terms and provides pairing correlations and the average mean field in a consistent fashion.

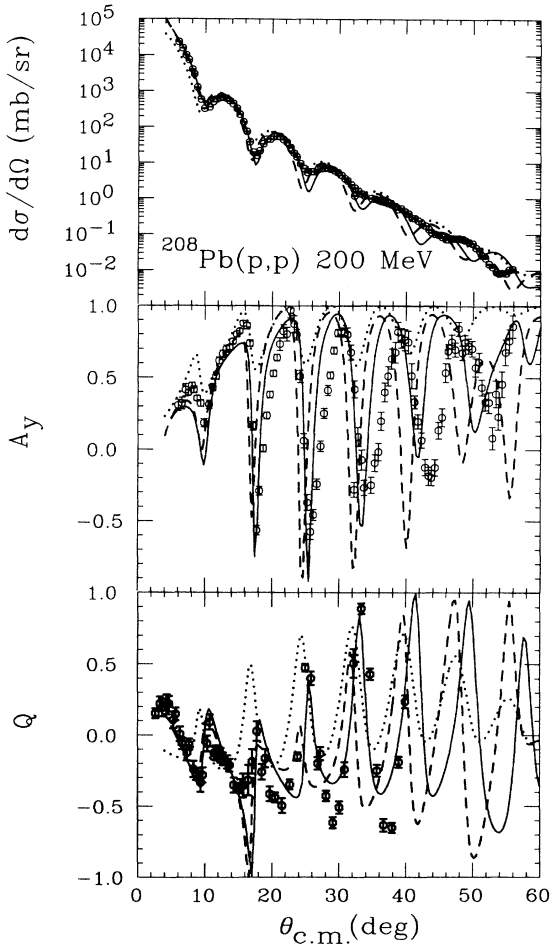

FIG. 3. Same as for Fig. 2, except that the target nucleus is ^{208}Pb. The data are from Ref. [21].

This fully microscopic mean-field theory using the D1S interaction has been shown to accurately describe static and dynamical properties of a range of nuclei [18]. We used Hartree-Fock-Bogoliubov densities because of our lack of knowledge about the neutron densities and our uncertainty about the validity of the usual prescription, in which the neutron and proton densities are taken to be identical. We note, however, that if we use this prescription, the elastic-scattering observables are not significantly changed for angles smaller than 40°.

The solid curves in Figs. 1–3 represent the proton-nucleus elastic-scattering calculations at 200 MeV with the Coulomb distortions taken into account as described in Secs. II and III; the dashed curves show the PW approximation. The dotted lines correspond to the complete omission of any Coulomb contributions altogether to illustrate the size of the effects discussed relative to the size of the entire Coulomb correction. From Fig. 1 it is evident that, for a light nucleus such as ^{16}O, the PW approximation is quite accurate even for larger angles, though it slightly overemphasizes the dip structure in the spin observables A_y and Q, as well as the minima in the differential cross section. This is different for heavier nuclei, as can be seen in Fig. 2, which shows the scattering observables for proton-nucleus elastic scattering from ^{40}Ca at 200 MeV. The angular distribution of the differential cross section shows that the PW approximation is slightly more diffractive than the exact calculation, a tendency which is again reflected in the fact that the PW approximation deepens the dip structure of the spin observables A_y and Q in the first minimum. We note further that, for angles larger than 40° the PW approximation differs considerably from the exact calculation. For very heavy nuclei like ^{208}Pb, the deficiencies of the PW approximation begin at $\sim 20°$. The angular distribution of the differential cross section shown in Fig. 3 indicates that the PW approximation squeezes the diffraction minima to smaller angles compared to the exact calculation. This mimics the effect of scattering from a larger nucleus, hence, the PW approximation somewhat misrepresents the physical size of a large nucleus. This effect is apparent as well in Figs. 1 and 2, but to a much lesser degree. The spin observables A_y and Q for elastic p-nucleus scattering from ^{208}Pb clearly indicate that, for this case, the PW approximation is inadequate even for smaller angles. Of particular interest is the curve for Q, where we see the crucial importance of the inclusion of Coulomb effects.

In Fig. 4 we plot the real part of the phase shift δ as a function of the orbital angular momentum L for proton scattering from ^{40}Ca at 200 MeV in order to characterize how the PW approximation may influence the interior wave function of the nucleus. We separate the cases $J=L+\frac{1}{2}$ and $J=L-\frac{1}{2}$ to isolate possible effects of the spin-orbit force. We also show the absolute value of the S matrix (η_l), which gives a measure of the absorptive character of the potential in each partial wave. As expected, different treatments of the Coulomb distortions do not alter the absorptive character of the optical potential. However, neglect of Coulomb distortions as in the PW approximation (dashed line versus solid line) underestimates the phase shift by $\sim 25\%$ for $L \leq 10$. Because the absorption is relatively strong in the low partial waves, the elastic-scattering observables shown in Fig. 2

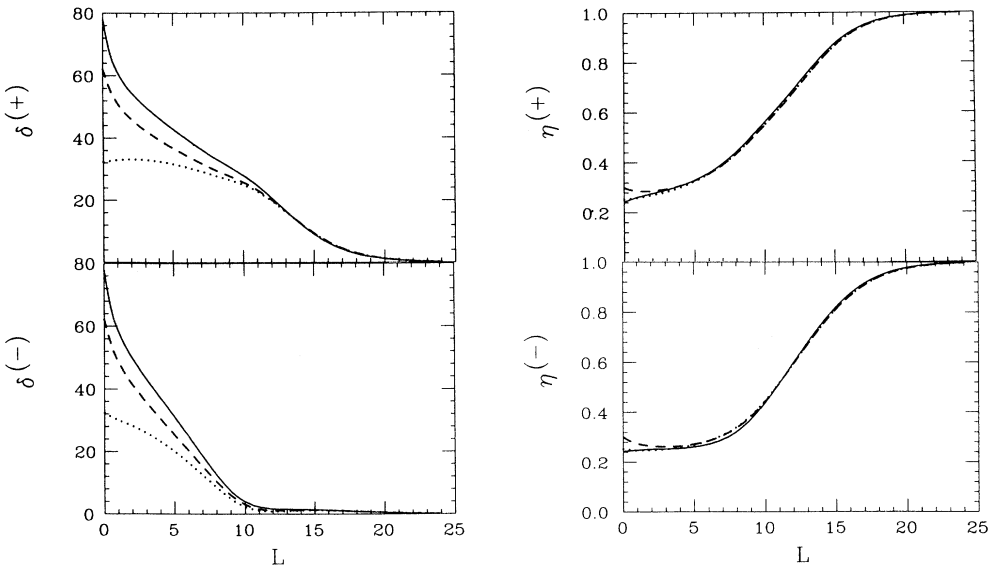

FIG. 4. The real part of the phase shift δ and absolute value of the S matrix η as functions of the orbital angular momentum L for scattering from ^{40}Ca at 200 MeV laboratory energy. The (+) denotes the phase shift for $J=L+\frac{1}{2}$, while the (−) stands for $J=L-\frac{1}{2}$. The solid line corresponds to the exact inclusion of the Coulomb distortions, the dashed line to the PW approximation, and the dotted line omits all Coulomb contributions. The calculation corresponds to the one in Fig. 2.

are not as sensitive to the PW approximation as could be concluded from the real part of the low partial-wave phase shifts shown in Fig. 4. It should be noted that, for $L > 10$, the Coulomb distorted waves become increasingly close to plane waves. This behavior suggests that, for high enough L at a given scattering energy, the PW approximation becomes very good. This is of considerable numerical advantage in the actual calculations. We found that, for very high partial waves, the Coulomb wave functions can safely be replaced by plane waves without loss of accuracy in the observables when evaluating the integral Eq. (42).

Because elastic scattering is strongly surface dominated, higher partial waves gain increasing relative importance at higher scattering energies. It can be expected that the PW approximation improves when increasing the energy. For our scattering calculation at 500 MeV, we start from an extension of the Bonn meson exchange interaction above pion production threshold, which is described in more detail in Ref. [3]. In Fig. 5 we show the scattering observables for elastic scattering from ^{40}Ca at 500 MeV laboratory energy. The solid curve represents the exact treatment of the Coulomb distortions, the dashed curve the PW approximation, while for the dotted curve all Coulomb contributions are omitted. The first-order optical potential has been calculated in the optimum factorized form. A comparison of the solid and dashed curves shows that the PW approximation is very close to the exact result for small angles. At angles larger than $\sim 30°$, the two calculations begin to deviate from one another. This improvement of the PW approximation can be understood by a comparison of the real parts of the phase shifts δ for both calculations (Fig. 6). Omitting the Coulomb distortions still underestimates the phase shifts (dashed versus solid line), but, in contrast to Fig. 4, the difference in magnitude between the two phase shifts is only about 15% for $L \leq 15$. Similar to the results at 200 MeV, the elastic-scattering observables are not as sensitive to these differences because of the strong absorptive character of the optical potential. In the case of proton scattering from ^{16}O at 500 MeV, we also find that the PW approximations is very close to the exact treatment of the Coulomb distortions.

So far we have established that the PW approximation is quite reliable for light nuclei in describing elastic-scattering observables for small angles and that its quality increases with increasing scattering energy. In order to see significant differences even at small angles, we have to go as low as 100 MeV laboratory energy. in Figs. 7 and 8 we present elastic-scattering observables for proton scattering from ^{40}Ca and ^{16}O at 100 MeV laboratory energy. The solid line shows the exact treatment of Coulomb distortions, the dashed line the PW approximation, and, for reference purposes, the dotted line omits all Coulomb contributions. Both targets show that, even at small angles, the PW approximation differs from the exact treatment of the Coulomb distortions. The effect is, in both cases, larger in A_y and Q than in the cross section, where there exist shifts in the spectrum as well as changes in the overall strength. However, it should be kept in mind that, at such a low energy, the concept of a first-order optical potential in impulse approximation is questionable. Certainly, medium modifications as well as higher-order terms in the multiple-scattering expansion are expected to give significant contributions.

All calculations above were carried out with a nonlocal optical potential in the optimum factorized form. Since the elastic observables show sensitivity to the treatment of Coulomb distortions for heavier nuclei, it is worthwhile investigating the size of the off-shell effects, which have been shown to be non-negligible, and determine if they are altered by the exact or approximate inclusion of Coulomb distortions. We have performed calculations with nonlocal optical potentials in the optimum factorized form (off-shell $\tau\rho$) and compared them with their local (on-shell $\tau\rho$) approximations. For details of the calculation of the optical potentials, we refer the

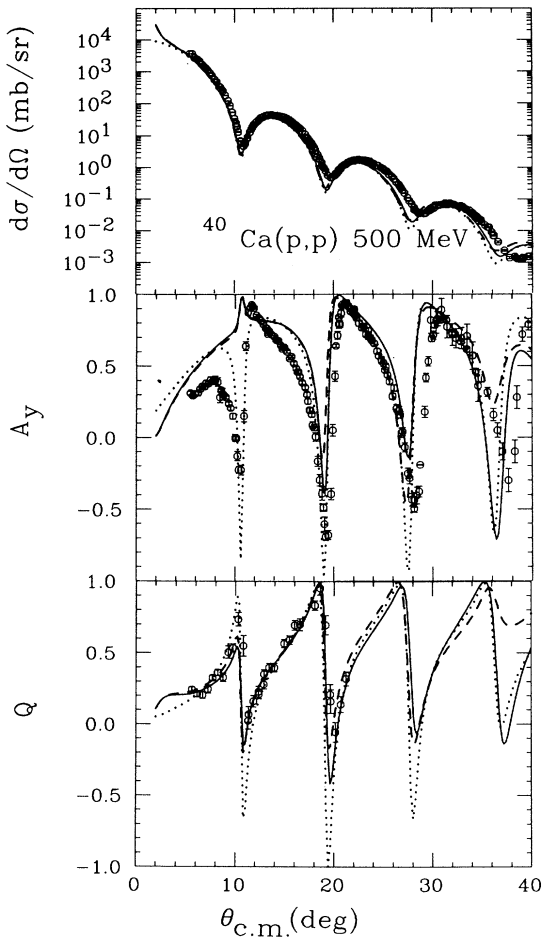

FIG. 5. The differential cross section, A_y, and Q for elastic proton scattering from ^{40}Ca at 500 MeV laboratory energy. The calculations with an exact treatment of the Coulomb distortions (solid) and the PW approximation (dashed) as well as the calculation which omits all Coulomb contributions (dotted) are based on the first-order optical potential in the optimum factorized form obtained from the Bonn NN model D52. The empirical data are from Ref. [22].

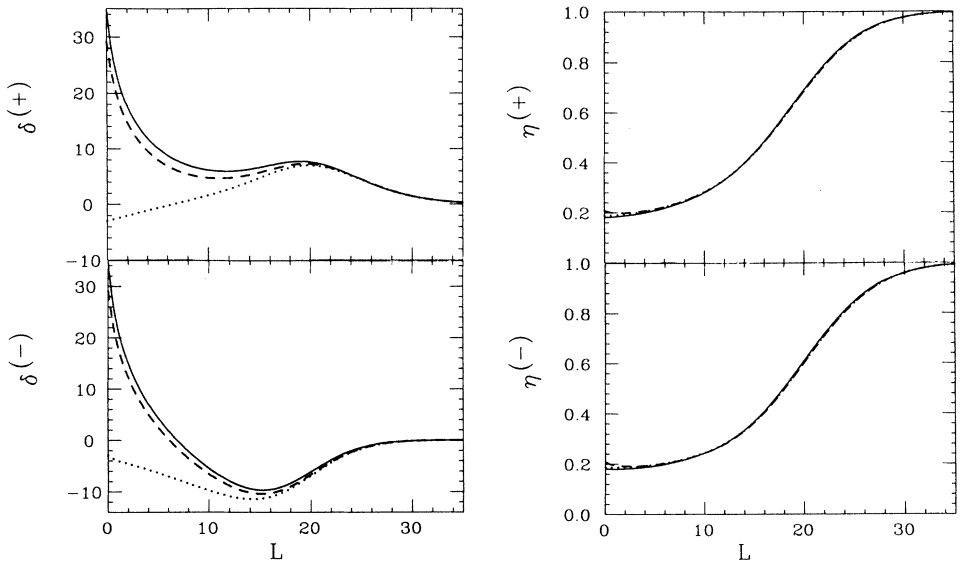

FIG. 6. The real part of the phase shift δ and absolute value of the S matrix η as functions of the orbital angular momentum L for scattering from ^{40}Ca at 500 MeV laboratory energy. The notations is the same as in Figs. 4 and 5.

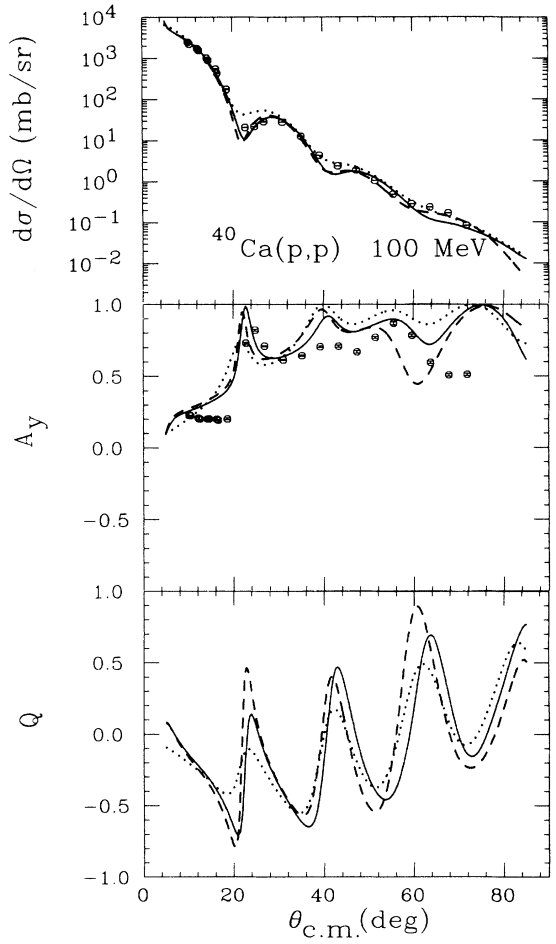

FIG. 7. The differential cross section, A_y and Q for elastic proton scattering from ^{40}Ca at 100 MeV laboratory energy. The calculations are performed with a first-order optical potential in the optimum factorized form obtained from the full Bonn interaction. The notation is the same as in Fig. 2, the empirical data are from Ref. [23].

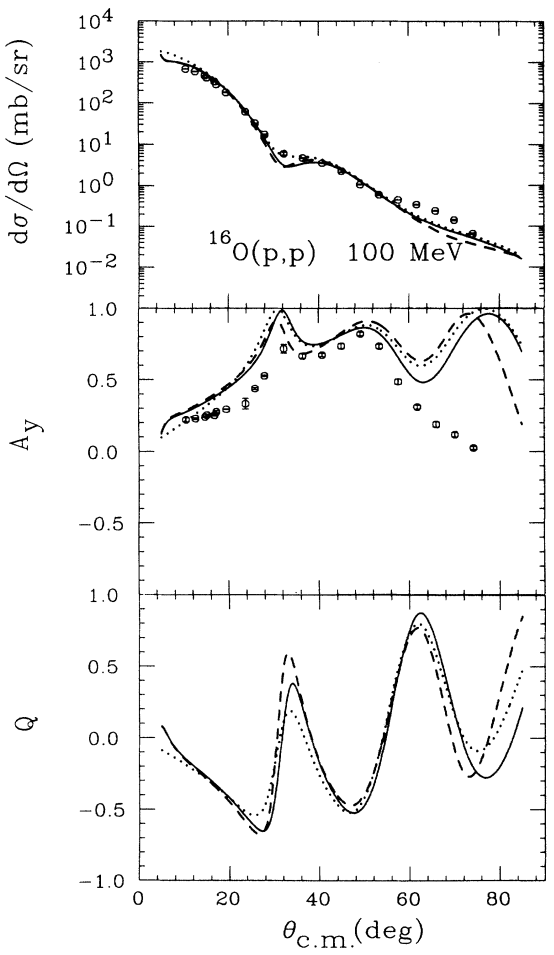

FIG. 8. The differential cross section, A_y, and Q for elastic proton scattering from ^{16}O at 100 MeV laboratory energy. The notation is the same as in Fig. 7, the empirical data are from Ref. [23].

reader to Refs. [3] and [4]. The observables for proton scattering from ^{40}Ca at 200 MeV are shown in Fig. 9. The off-shell effects are quite noticeable and very similar in size and character to those found in Ref. [3], where the PW approximation had been applied. We stated above that the PW approximation shifts the diffraction minima to slightly smaller angles. This was consistently observed for all off-shell and on-shell cases we studied. The convolution with plane waves instead of Coulomb wave functions [Eq. (37)] does not change the off-shell character of the optical potential.

In Fig. 10 we display the off-shell dependence for proton elastic scattering from ^{208}Pb at 200 MeV. Here the off-shell effects are relatively small at forward angles, in contrast to the lighter nucleus ^{40}Ca. They start to be visible only at the third minimum in Q. Since Coulomb distortions play a significant role for ^{208}Pb, we show the spin observables A_y and Q calculated without Coulomb distortions in Fig. 11. Here, off-shell effects are visible in Q at the first minimum. Clearly, because of the high charge, the proton-nucleus spin observables are dominated by the Coulomb force in the forward direction, masking the off-shell effects at small angles.

V. SUMMARY

We have performed calculations for elastic proton scattering from different nuclei up to 500 MeV laboratory energy with nonlocal and first-order optical potentials. Since the long-ranged Coulomb force and the strong, short-ranged nuclear interactions must be treated differently in multiple scattering, we derived the first-order term within the Watson formalism. Using the two-potential formula, we separated out the point Coulomb part and isolated the short-range contribution in a Coulomb distorted term. This separation gives the

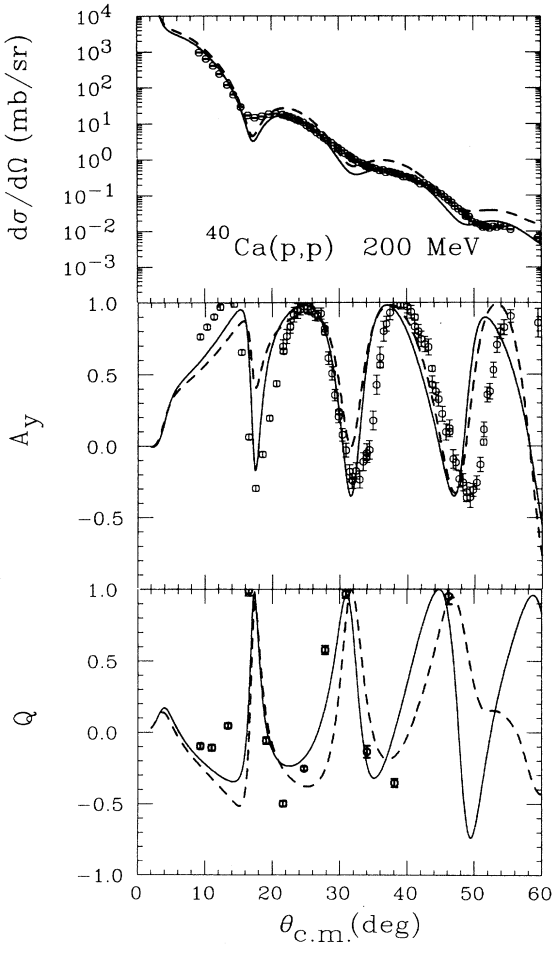

FIG. 9. The differential cross section, A_y, and Q for elastic proton scattering from ^{40}Ca at 100 MeV laboratory energy. The calculations include Coulomb distortions exactly and are with a first-order optical potential obtained from the full Bonn interaction in the on-shell local approximation (dashed curve) and with off-shell nonlocal effects included (solid curve). The data are from Ref. [20].

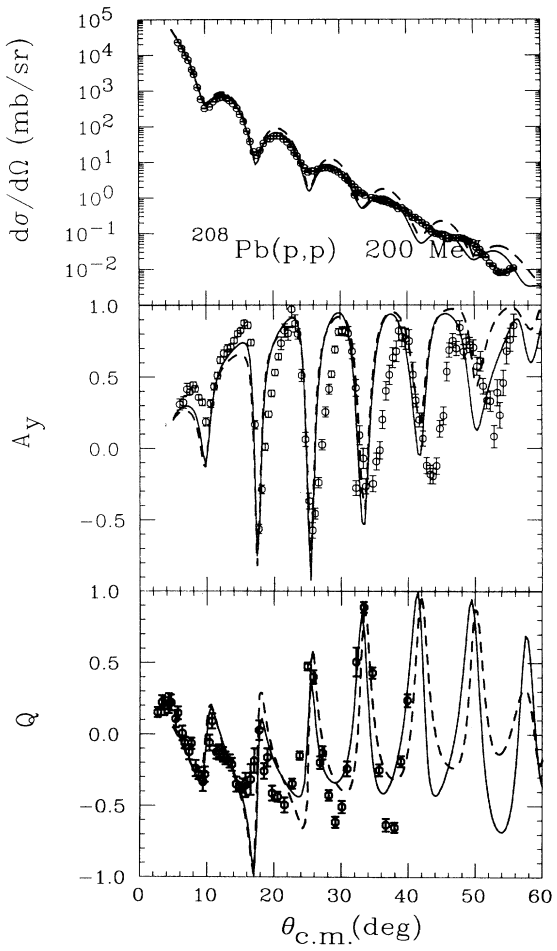

FIG. 10. The differential cross section, A_y, and Q for elastic proton scattering from ^{208}Pb at 200 MeV laboratory energy. The calculations shown are the off-shell (solid line) and on-shell (dashed line) results from the first-order optical potential with Coulomb distortions included exactly. The data are from Ref. [21].

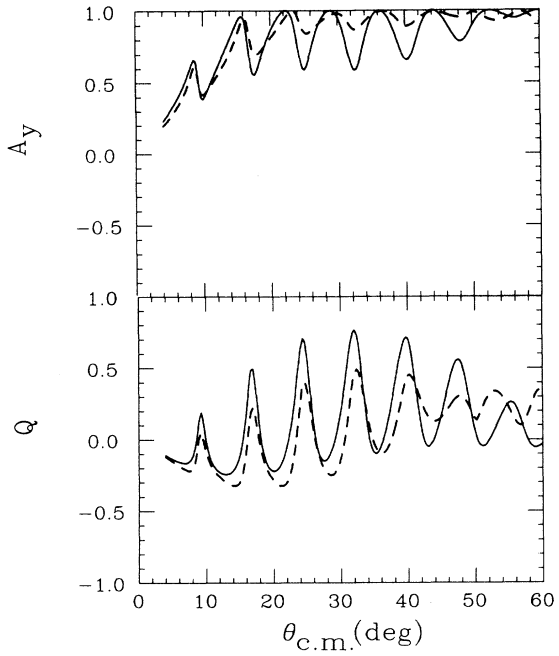

FIG. 11. Same as for Fig. 10 for A_y and Q except here both the off-shell (solid line) and on-shell (dashed line) calculations omit all Coulomb contributions.

Rutherford scattering amplitude in the extreme limit in which the short-range potential W is ignored as well as the correct distributed Coulomb amplitude, when the nuclear interaction is neglected. The Coulomb distorted nuclear matrix elements are calculated in momentum space in an *exact* and numerically stable manner. We have compared our exact results for ^{16}O, ^{40}Ca, and ^{208}Pb to the PW approximation, which replaces the Coulomb distorted nuclear matrix element by a plane-wave matrix element in the two potential formula. We determined that the PW approximation is well suited for describing elastic-scattering observables for light nuclei in the forward direction, and it improves with increasing energy. In a more detailed analysis of the elastic-scattering calculation, we found that the Coulomb distortions are very significant in low partial waves, and that they decrease in magnitude with increasing orbital angular momentum. This is evident from the figures which display the phases and magnitudes of the S matrix as a function of the orbital angular momentum.

The general trend is that the PW approximation squeezes the diffraction pattern of the differential cross section and consequently of the spin observables and thus mimics a target nucleus of larger size. This is especially evident in the elastic-scattering observables for ^{208}Pb and makes the PW approximation clearly inadequate for large-Z nuclei.

We further investigated whether the correct treatment of the Coulomb distortions influences the size of nonlocality effects in the nuclear optical potential. For light nuclei (up to ^{40}Ca), we found a very small dependence of the size of off-shell effects on the treatment of Coulomb distortions. The effect is found to be nearly the same as reported in Ref. [2]. Furthermore, the size of the effect is the same whether nonlocal optical potential is obtained from the full-folding integral or whether the optimum factorized form is used. As long as the nuclear charge is small, off-shell effects are larger than effects induced by approximate treatments of Coulomb distortions. This is no longer true if the nuclear charge is large. The spin observables in the forward direction for ^{208}Pb are dominated by the Coulomb distortions and nonlocal effects play only a less important role. Their influence only becomes visible at larger angles.

In conclusion, we have provided an exact procedure for treating the Coulomb interaction in a first-order Watson-type multiple-scattering expansion and have used this to find the range of validity of the PW approximation of Ref. [13].

ACKNOWLEDGMENTS

The authors acknowledge financial support from the National Science Foundation under Grants Nos. PHY-8858250 and PHY-8822550. This work was performed partially under the auspices of the U.S. Department of Energy by the Lawrence Livermore National Laboratory under Contract No. W-7405-ENG-48. The computational support of the Ohio Supercomputer Center under Grant No. PDS150 and the Open Computing Facility of the Livermore Computer Center is gratefully acknowledged. The authors want to thank P.C. Tandy and R. J. Perry for valuable discussions and critical reading of the manuscript.

[1] H. F. Arellano, F. A. Brieva, and W. G. Love, Phys. Rev. Lett. **63**, 605 (1989); Phys. Rev. C **41**, 2188 (1990).
[2] R. Crespo, R. C. Johnson, and J. A. Tostevin, Phys. Rev. C **41**, 2257 (1990).
[3] Ch. Elster and P. C. Tandy, Phys. Rev. C **40**, 881 (1989).
[4] Ch. Elster, T. Cheon, E. F. Redish, and P. C. Tandy, Phys. Rev. C **41**, 814 (1990).
[5] C. M. Vincent and S. C. Phatak, Phys. Rev. C **10**, 391 (1974).
[6] R. Crespo and J. A. Tostevin, Phys. Rev. C **41**, 2615 (1990).
[7] N. Ottenstein, E. E. van Faassen, J. A. Tjon, and S. J. Wallace, Phys. Rev. C **42**, 1825 (1990); University of Maryland Report No. 90-091, 1991.
[8] Ch. Elster, L. C. Liu, and R. M. Thaler, Los Alamos National Laboratory Report LA-UR-90-2126, 1990; and unpublished.
[9] K. M. Watson, Phys. Rev. **89**,d 575 (1953).
[10] A. K. Kerman, H. McManus, and R. M. Thaler, Ann. Phys. (N.Y.) **8**, 551 (1959).
[11] L. Ray, G. W. Hoffmann, and R. M. Thaler, Phys. Rev. C **22**, 1554 (1980).

[12] M. A. Nagarajan, W. L. Wang, D. E. Ernst, and R. M. Thaler, Phys. Rev. C **11**, 1167 (1975).
[13] A. Pickelsimer, P. C. Tandy, R. M. Thaler, and D. H. Wolfe, Phys. Rev. C **30**, 2225 (1984).
[14] P. C. Tandy, E. F. Redish, and D. Bollé, Phys. Rev. C **16**, 1924 (1977).
[15] E. F. Redish and K. Stricker-Bauer, Phys. Rev. C **36**, 513 (1987).
[16] R. Machleidt, K. Holinde, and Ch. Elster, Phys. Rep. **149**, 1 (1987).
[17] C. W. DeJaeger, M. De Vries, and C. De Vries, Nucl. Data Tables **14**, 479 (1974).
[18] See, for example, J.-F. Berger, M. Girod, and D. Gogny, Nucl. Phys. **A502**, 85 (1989); J. P. Delaroche, M. Girod, J. Libert, and I. Deloncle, Phys. Lett. B **232**, 145 (1989).
[19] J.-F. Berger, M. Girod, and D. Gogny, Comput. Phys. Commun. **63**, 365 (1991).
[20] E. J. Stephenson, in *Antinucleon- and Nucleon-Nucleus Interaction,* edited by G. Walker, C. D. Goodman, and C. Olmer (Plenum, New York, 1985), p. 299.
[21] D. A. Hutcheon *et al.,* in *Polarization Phenomena in Nuclear Physics—1980 (Fifth International Symposium, Santa Fe),* Proceedings of the Fifth International Symposium on Polarization Phenomena in Nuclear Physics, AIP Conf. Proc. No. 69, edited by G. G. Ohlson, R. E. Brown, N. Jarmie, W. W. McNaughton, and G. M. Hale (AIP, New York, 1981), p. 454. The data for Q are from Na Gi, Masters Thesis, Simon Fraser University, British Columbia, 1987.
[22] G. W. Hoffmann *et al.,* Phys. Rev. Lett. **47**, 1436 (1981); A. Rahbar *et al., ibid.* **47**, 1811 (1981).
[23] H. Siefert, Ph. D. thesis, University of Maryland, 1990.